remote sensing

Article

Long-Term Temporal and Spatial Monitoring of Cladophora Blooms in Qinghai Lake Based on Multi-Source Remote Sensing Images

Hongyu Duan [1], Xiaojun Yao [1,*], Dahong Zhang [2], Huian Jin [1,3] and Qixin Wei [1]

1 College of Geography and Environment Science, Northwest Normal University, Lanzhou 730070, China; 2020120154@nwnu.edu.cn (H.D.); 2018222406@nwnu.edu.cn (H.J.); 2020212719@nwnu.edu.cn (Q.W.)
2 College of Urban and Environmental Science, Northwest University, Xi'an 710127, China; zhangdahong@stumail.nwu.edu.cn
3 College of Forestry Engineering, Gansu Forestry Polytechnic, Tianshui 741020, China
* Correspondence: xj_yao@nwnu.edu.cn; Tel.: +86-131-0930-9241

Abstract: With climate warming and intensification of human activities, the eco-environmental problems of lakes in middle and high latitudes become increasingly prominent. Qinghai Lake, located in the northeastern of the Tibetan Plateau, is the largest inland saltwater lake in China. Recently, the problem of Cladophora blooms has been widely concerning. In this study, the area of floating Cladophora blooms (hereafter FCBs) in Qinghai Lake from 1986 to 2021 was extracted using Floating Algal Index (FAI) method based on Landsat TM/ETM+/OLI and Sentinel-2 MSI images, and then the intra- and inter-annual variation characteristics and spatial patterns of FCBs were analyzed. The results show that the general change trend of FCBs in Qinghai Lake featured starting in May, expanding rapidly from June to August, and increasing steadily from September to October. From 1986 to 2021, the area of FCBs in Qinghai Lake showed an overall increasing trend in all months, with the largest increase in July at 0.1 km^2/a, followed by October at 0.096 km^2/a. Spatially speaking, the FCBs area showed a significant increasing trend in the northern Buha River estuary (BRN) and southern Buha River estuary (BRS) regions, a slight increase in the Shaliu River estuary (SR) region, and a decreasing trend in the Quanji River estuary (QR) region and the Heima River estuary (HR) region. The correlation between the meteorological factors and the changes in FCBs was weak, but the increase in flooded pastures in the BRN region (Bird Island) due to rising water levels was definitely responsible for the large-scale increase in FCBs in this region. However, the QB, northeastern bay of Shaliu River estuary (SRB) and HR regions, which also have extensive inundated grassland, did not have the same increase in FCBs area, suggesting that the growth of Cladophora is caused by multiple factors. The complex relationships need to be verified by further research. The current control measures have a certain inhibitory effect on the Cladophora bloom in Qinghai Lake because the FCBs area was significantly smaller in 2017–2020 (5.22 km^2, 3.32 km^2, 4.55 km^2 and 2.49 km^2), when salvage work was performed, than in 2016 and 2021 (8.67 km^2 and 9.14 km^2), when no salvage work was performed.

Keywords: floating Cladophora blooms; spatial and temporal patterns; remote sensing; Qinghai Lake

check for updates

Citation: Duan, H.; Yao, X.; Zhang, D.; Jin, H.; Wei, Q. Long-Term Temporal and Spatial Monitoring of Cladophora Blooms in Qinghai Lake Based on Multi-Source Remote Sensing Images. *Remote Sens.* **2022**, *14*, 853. https://doi.org/10.3390/rs14040853

Academic Editors: Junsheng Li, Gongliang Yu, Chen Wang and Yao Liu

Received: 18 November 2021
Accepted: 27 January 2022
Published: 11 February 2022

1. Introduction

As a crucial part of global water resources, lakes play an essential role in water cycle, climate regulation and biodiversity conservation [1]. In recent years, the dual effects of natural and human activities have caused drastic changes in lake water environment, resulting in continuous deterioration of water quality and severe damage to the ecosystem [2]. One of the main manifestations is the eutrophication-led algal blooms, for example, with 68% of 71 large lakes worldwide having experienced a significant trend of increasing intensity of blooms [3]. Lake Erie [4] in the United States, Lake Winnipeg in Canada [5], Lake Taihu [6], Lake Chaohu [7] and Lake Dianchi [8] in China have all been terribly affected by algal blooms. China has become one of the countries with the most serious and widespread algal blooms in the world [9]. Qinghai Lake is the largest inland saltwater lake in China, which is a vital water resource for maintaining ecological security in the northeastern Tibetan Plateau. On 8 June 2021, the top Chinese leader visited this lake and emphasized the importance of protecting its ecological environment. Currently, the general nutrient level in Qinghai Lake remains relatively stable [10]; however, the continuous rising water levels since 2005 and the intensified human activities in the surrounding areas have led to the emergence of some ecological problems, such as the Cladophora blooms on the near-shore waters of the western and northern parts of Qinghai Lake, impacting the landscape and ecological environment [11].

There are many algal blooms-related studies on lake Taihu [1,12], Lake Chaohu [13,14] and Lake Dianchi [15,16] in southern China, as well as Lake Wuliangsuhai [17,18], the Yuqiao Reservoir [19,20], Lake Hulun and Lake Bel [21] in northern China, but fewer studies on Qinghai Lake. Before 2000, researchers from the Institute of Hydrobiology, Chinese Academy of Sciences, and the Qinghai Lake Comprehensive Survey reported and recorded Cladophora blooms in some bays and near regions of river estuaries in Qinghai Lake [22,23]; Yang et al. [24] clarified that Cladophora was the dominant species of benthic algae in Qinghai Lake and estimated the amount of Cladophora. After 2000, Yao et al. [25] found fewer Cladophora blooms in Qinghai Lake in 2006–2010 and believed that there was a shrinking trend. Hao et al. [11] deemed that the water quality did not change significantly, but the Cladophora biomass was considerable, and the Cladophora blooms' area was positively correlated with water levels in 2011–2019. Zhao et al. [26] designated the Cladophora in Qinghai Lake as a new species of Cladophora Qinghaiensis sp. nov., based on morphological characters and molecular phylogenetic analysis. Although previous studies identified the existence of Cladophora blooms in Qinghai Lake and analyzed some of the changes, there has been a gap in systematic analysis and research on the spatial and temporal patterns of Cladophora blooms in Qinghai Lake over a long-term series.

Remote sensing technology has been widely used for monitoring the location, area and dynamic of algal blooms due to its wide range, fast speed, low cost and high repeatability [27], based on the main principle that water body covered by phytoplankton blooms exhibits a special spectral feature of low reflection in red band and high reflection in green and near-infrared (NIR) bands [2]. Current methods commonly used for monitoring algal blooms include the single band method, based on the "lift effect" in NIR band, the difference method, ratio method, normalized difference vegetation index (NDVI), enhanced vegetation index (EVI), floating algae index (FAI), based on reflectance difference among visible bands, NIR bands and SWIR bands [28–31]. In addition, there are some methods of monitoring phytoplankton pigments, such as cyanobacteria bloom algae index (CAI), maximum characteristic peak height (MPH) method and maximum chlorophyll index (MCI) [32–34]. Cladophora blooms in Qinghai Lake are relatively small in area and mainly distribute in estuaries and coastal regions; therefore, the MODIS product with outstanding effectiveness for monitoring algal blooms is unavailable. Landsat series images have the advantage of long-time span and higher spatial resolution (15–30 m) for monitoring algal blooms in Qinghai Lake. One shortcoming is fewer available images during the algal bloom growth period because of a longer revisit cycle (16 days). Sentinel-2 MSI imagery began in 2015 with the spatial resolution of 10 m and a revisit cycle of 5 days, which can be used as an effective data source for monitoring Cladophora blooms in Qinghai Lake. Therefore, the aim of this study is to extract the long-term Cladophora blooms' area in Qinghai Lake, based on Landsat TM/ETM+/OLI and Sentinel-2 MSI images, using the widely adopted FAI method, and then analyze the temporal and spatial variation characteristics of Cladophora blooms in Qinghai Lake to promote the understanding and mastery of Cladophora blooms, as well as to provide data support and theoretical reference for the control and governance in the future.

2. Study Area

Qinghai Lake (36°32′–37°14′N, 99°36′–100°46′E), located in the semi-arid alpine climate zone, is a significant water body for maintaining ecological security in the northeastern Tibetan Plateau (Figure 1a), as well as being an important plateau lake for concentrated breeding of waterfowls and a famous tourist destination nationwide. As the largest inland saltwater lake in China, its water levels have declined gradually from the 1950s, then rebounding since 2004 with a dramatic area expansion [35,36], which was about 4543 km^2 in late April 2020. There are more than 40 rivers of different sizes in the basin, with larger runoff rivers located in the northwestern part of the lake. Since the 1980s, tourism has been on the rise at Qinghai Lake. Water ecology has remained generally stable amidst the background of climate warming. However, the presence of Cladophora blooms in some regions, such as the Shaliu River estuary (SR) and its northeastern bay (SRB), the Quanji River estuary (QR), the northern Buha River estuary (BRN) (Bird Island) and southern Buha River estuary (BRS), the Quan Bay (QB) and the Heima River estuary (HR), has caused significant impact on the wetland ecosystem and the beautiful scenery of Qinghai Lake (Figure 1b).

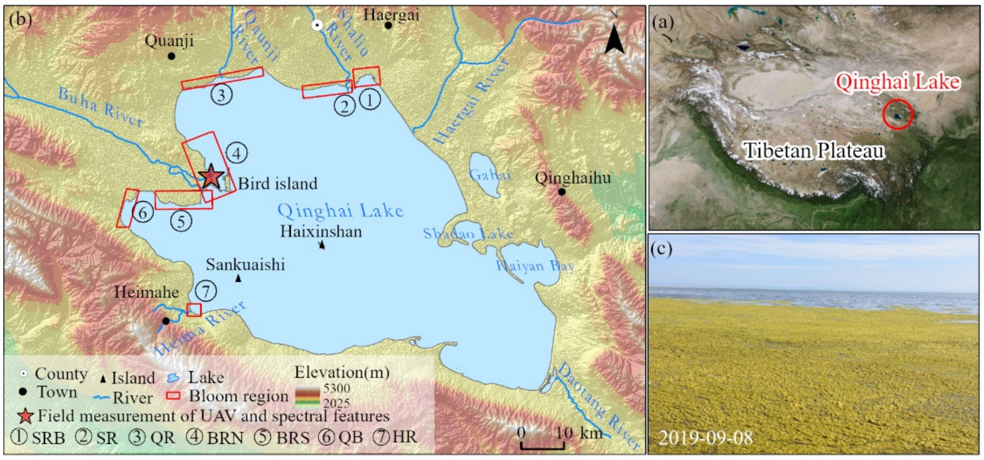

Figure 1. Overview of study area. (**a**) Location of Qinghai Lake in the Tibetan Plateau. (**b**) Description of the study regions and the sampling location in the Qinghai Lake. (**c**) Photo of floating Cladophora blooms near the northern Buha River estuary region.

Cladophora in Qinghai Lake has nucleated tubular cells and branched or unbranched filaments, which are typical benthic attached algae that can grow on stable substrates for many years and widely distribute in rivers, lakes and shallow offshore waters [37]. Cladophora can contribute to the biochemical cycle of aquatic ecosystems, increase the hierarchy of aquatic ecosystems and enhance species diversity. However, its overgrowth has negative effects, such as inhibiting growth of other submerged plants, deteriorating water quality, releasing unpleasant odors and affecting landscapes [38] (Figure 1c). Cladophora in Qinghai Lake can be classified into two forms: the attaching type and the floating type. When the attached type reaches a certain biomass, the plant body breaks and floats under the action of wind and waves, forming the yellow-green-colored floating Cladophora blooms (hereafter FCBs), which can be clearly identified by remote sensing images and are the analysis object of this study.

2.1. Materials and Pre-Processing

The combined use of multiple satellite data in the analysis of spatial and temporal variability of algal blooms in long time series can help overcome deficiencies of short coverage time, long repetition period and lack of available data caused by a single satellite. In this study, multi-source data were used to accurately extract FCBs area in Qinghai Lake in the long term. Among them, Landsat TM/ETM+/OLI and Sentinel-2 MSI images were used to extract the FCBs area from 1986–2017 and 2016–2021, respectively; Unmanned Aerial Vehicle (UAV) image was used to verify the extraction accuracy of the FCBs area; field-measured spectral data of Cladophora blooms was used to assist in selecting the extraction method; and meteorological data from the Guncha station and land use and land cover (LULC) data of GLC_FCS30 (https://data.casearth.cn/, accessed on 18 November 2021) was used to assist in the analysis of the driving forces of Cladophora blooms in Qinghai Lake. It is worth noting that except for 2018, 2020 and 2021, no other years have images available that fully cover the May-October period; 1995, 2017 and 2019 are only missing images from certain months, and 1987, 1990, 1992, 1997, 2000, 2001, 2006, 2010, 2015 and 2016 have four images available, including at least July or August and September or October. These images were used to analyze the intra-annual variability characteristics of FCBs in Qinghai Lake. Additionally, there were no images available in 1988 and 2012 due to heavy clouds. A total of 192 scenes of Landsat Level-1 images (Orbit: 133/034 and 133/035) from 1986 to 2021 were acquired from the United States Geological Survey (USGS) website (https://earthexplorer.usgs.gov/, accessed on 18 November 2021) (Table 1), and these images were radiometrically calibrated and atmospherically corrected using the ENVI 5.3 software. Meanwhile, Landsat ETM+/OLI pan-sharpened image with a spatial resolution of 15 m was created by band fusion in ArcGIS 10.4 software. There were 109 scenes of cloud-free Sentinel-2 MSI images covering Qinghai Lake from 2016 to 2021, which were downloaded from the European Space Agency website (http://scihub.copemicus.eu/, accessed on 18 November 2021). Both Level-2A images and Level-1C images are included. The former are radiometrically calibrated and atmospherically refined reflectance data at the bottom of the atmosphere; the latter are top-of-atmosphere (TOA) reflectance data, which were atmospherically corrected and geometrically fine corrected using the Sen2cor processing module of Sentinel Application Platform (SNAP) in this study. Otherwise, the Super-Resolution Synthesis process was performed for band 8A (NIR) and band 11 (SWIR) (spatial resolution being 20 m) for all images using the Sen2Res plug-in of SNAP in order to yield images with a spatial resolution of 10 m and a better texture characteristic than the general resampling processing could render.

Table 1. Landsat TM/ETM+/OLI and Sentinel-2 MSI images used in this study.

Year	Month					
	May	June	July	August	September	December
1986	—	06/09 [T]	—	—	—	10/31 [T]
1987	—	06/28 [T]	—	08/15 [T]	09/16 [T]	10/02 [T]
1989	05/16 [T]	06/01 [T]	—	—	09/21 [T]	—
1990	—	06/20 [T]	—	08/23 [T]	—	10/10 [T]
1991	—	—	07/09 [T]	—	—	10/29 [T]
1992	—	06/09 [T]	—	08/28 [T]	09/04 [T]	10/15 [T]
1993	05/27 [T]	06/28 [T]	—	08/31 [T]	—	—
1994	—	—	—	—	—	10/21 [T]
1995	05/17 [T]	06/18 [T]	—	08/21 [T]	09/22 [T]	10/08 [T]
1996	05/19 [T]	06/20 [T]	—	—	09/08 [T]	10/26 [T]
1997	05/22 [T]	06/23 [T]	—	08/26 [T]	—	10/29 [T]
1998	—	06/26 [T]	07/28 [T]	—	—	—
1999	—	—	07/31 [T]	08/08 [E]	—	10/27 [E]
2000	05/14 [T]	06/15 [T]	—	08/18 [T]	—	10/05 [T]
2001	05/09 [E]	06/18 [T]	—	08/21 [T]	—	10/24 [T]
2002	—	06/05 [T]	—		—	10/11 [T]
2003	—	—	—		09/12 [T]	—
2004	—	—	—		09/14 [T]	—
2005	—	06/29 [T]	07/15 [T]	—	09/17 [T]	—
2006	05/31 [T]	06/16 [T]	—	08/03 [T]	09/20 [T]	—
2007	05/18 [T]	—	—	—	—	—

Table 1. *Cont.*

Year	Month					
	May	June	July	August	September	December
2008	05/04 T	06/05 T	07/23 T	—	—	—
2009	—	—	—	08/11 T	09/28 T	10/30 T
2010	05/10 T	—	07/29 T	08/14 T	—	10/17 T
2011	—	06/14 T	07/16 T	—	—	10/04 T
2013	—	—	—	—	09/23 E	10/09 E
2014	05/21 O	06/06 O	07/24 O	08/25 O	—	—
2015	—	—	07/27 O	08/12 O	09/13 O	10/15 O
2016	05/11 M	06/27 O	07/30 M	—	—	10/17 O
2017	05/29 O	06/30 O	07/15 M	08/04 M	—	10/04 O
2018	05/10 M	06/10 M	07/30 M	08/19 M	09/28 M	10/03 M
2019	—	06/05 M	07/05 M	08/14 M	09/28 M	10/28 M
2020	05/05 M	06/29 M	07/14 M	08/18 M	09/02 M	10/07 M
2021	05/05 M	06/04 M	07/29 M	08/28 M	09/07 M	10/02 M

Note: Superscripts T, E, O, M represent the images of Landsat TM, Landsat ETM+, Landsat OLI and Sentinel-2 MSI, respectively.

The UAV image covering the BRN region (Bird Island) in Qinghai Lake (Figure 1) was taken by a DJI AFI 4 drone on 6 September 2019 and 23 July 2021 with the spatial resolution of 5 cm, geographic coordinate system of WGS1984 and map projection of UTM. The flight altitude and speed of the drone were 185 m and 9.5 m/s, respectively. Post-processing was carried out using Pix4Dmapper software, producing an accurate 2D image with geographic coordinate system and map projection of WGS1984 and UTM to check the accuracy of the FAI-extracted FCBs area. The spectral features of Cladophora blooms in Qinghai Lake were measured by a field portable SVC (Spectra Vista Corporation, USA) spectroradiometer in the BRN region (Figure 1) at 13:00–14:00 on 6 September 2019 (Figure 2a). The spectral reflectance was calibrated by a dedicated flat whiteboard, and the spectroradiometer was vertically one meter away from the water surface. Then, the field-measured spectral reflectance was normalized using the average spectral reflectance from 350 to 1050 nm to reduce the influence of the external environment Equation (1) and highlight the characteristic of the spectral profile (Figure 2b):

$$R_N(\lambda_i) = \frac{R(\lambda_i)}{\frac{1}{n}\sum\limits_{350}^{1050} R(\lambda_i)} \quad (1)$$

where $R_N(\lambda_i)$ is the normalized reflectance of FCBs, $R(\lambda_i)$ is the field-measured reflectance of FCBs, n is the number of bands in the range of spectral reflectance between 350–1050 nm.

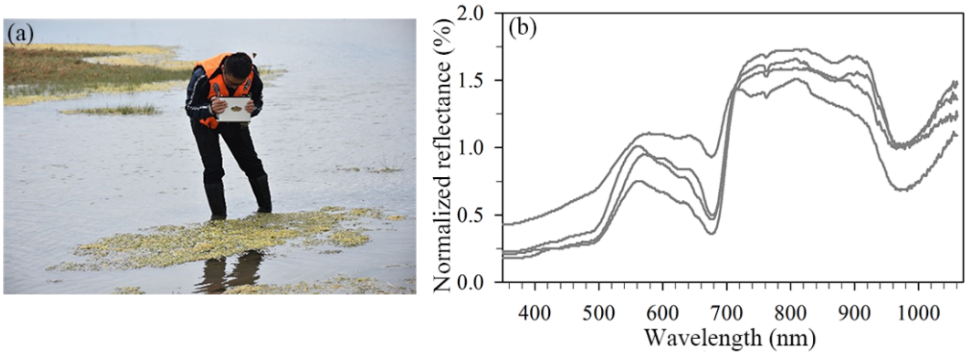

Figure 2. (**a**) Acquisition of spectral data of Cladophora blooms in Qinghai Lake and (**b**) the normalized spectral features by average reflectance in the range of 350~1050 nm.

2.2. Methods

2.2.1. Land Masking

Algae have similar spectrum characteristics to vegetation, and pixels of land surface have high FAI values [20], thus they should be excluded. The multi-period water boundaries of Qinghai Lake were firstly extracted using normalized difference water index (NDWI):

$$NDWI = (R_g - R_{nir})/(R_g + R_{nir}) \quad (2)$$

where, R_g and R_{nir} are reflectance in green and NIR bands, corresponding to band 2 and band 4 of Landsat TM images, band 3 and band 5 of Landsat ETM+/OLI images and band 3 and band 8A of Sentinel-2 MSI images. Then, the results were carefully visually inspected and revised to obtain accurate land masks. Finally, the water boundaries were retracted by one pixel width (30 m for Landsat TM images, 15 m for Landsat ETM+/OLI images and 10 m for Sentinel-2 MSI images) toward water body to avoid the adjacent land effect [12,39,40].

2.2.2. FCBs Extraction

Field-measured spectral data indicate that FCBs in Qinghai Lake have typical spectral characteristics of high reflectance in green band, as well as the "lift-effect" in NIR band (Figure 2b). Hu et al. [31] invented the FAI method based on a combination of red, NIR and SWIR bands to monitor algae in sea, which has the advantages of low sensitivity and high stability and has been widely used for monitoring algae blooms in lakes [41,42]. In this study, the FAI method Equations (3) and (4) was applied to the initial extraction of FCBs:

$$FAI = R_{nir} - R'_{nir} \quad (3)$$

$$R'_{nir} = R_{red} + (R_{swir} - R_{red}) \times (\lambda_{nir} - \lambda_{red})/(\lambda_{swir} - \lambda_{red}) \quad (4)$$

where, R_{red} (λ_{red}), R_{nir} (λ_{nir}) and R_{swir} (λ_{swir}) are reflectance and central wavelengths of red, NIR and SWIR bands, respectively, corresponding to band 3 (0.66 μm), band 4 (0.83 μm) and band 5 (1.65 μm) for Landsat TM images, band 4 (0.66 μm), band 5 (0.87 μm) and band 6 (1.61 μm) for Landsat ETM+/OLI images and band 4 (0.67 μm), band 8A (0.87 μm) and band 11 (1.61 μm) for Sentinel-2 MSI images. R'_{nir} is the interpolated reflectance, namely, the reflectance obtained by linear interpolation at NIR band based on red and SWIR bands.

In this study, the optimal threshold for FAI method for extracting FCBs was determined by the threshold iteration method (with a step of 0.01). With a threshold of 0.3–0.5, the FAI method can essentially extract the FCBs accurately. The improperly extracted parts were then checked and revised manually, based on true color composite images.

3. Results

3.1. The Change of FCBs

3.1.1. Intra-Annual Change

Based on the available remote sensing images, the intra-annual change of FCBs in Qinghai Lake showed different variation patterns. In 1987, 1990, 2000, 2006, 2010, 2015, 2017 and 2021, the area of FCBs had a gradual increase from May to October (Figure 3). In 1992 and 1995, the FCBs peaked in August and September, and then moderately decreased in October. Conversely, in 1997, 2001, 2016 and 2019, the maximum area of FCBs was observed in July or August, with a greater decrease in October. The changes in 2018 and 2020 were unique. There was a large area in August 2018 and a larger area in October than in August, after a decrease in September. In 2020, the maximum area of FCBs occurred in August, but the area in July was slightly smaller than in June (Figure 3), which may be caused by the artificial salvage treatment. In general, a comprehensive analysis of different months over a long term shows that the FCBs area in Qinghai Lake is characterized by the beginning of May, with rapid expansion from June to August and a steady increase from September to October, which is obtained in most years.

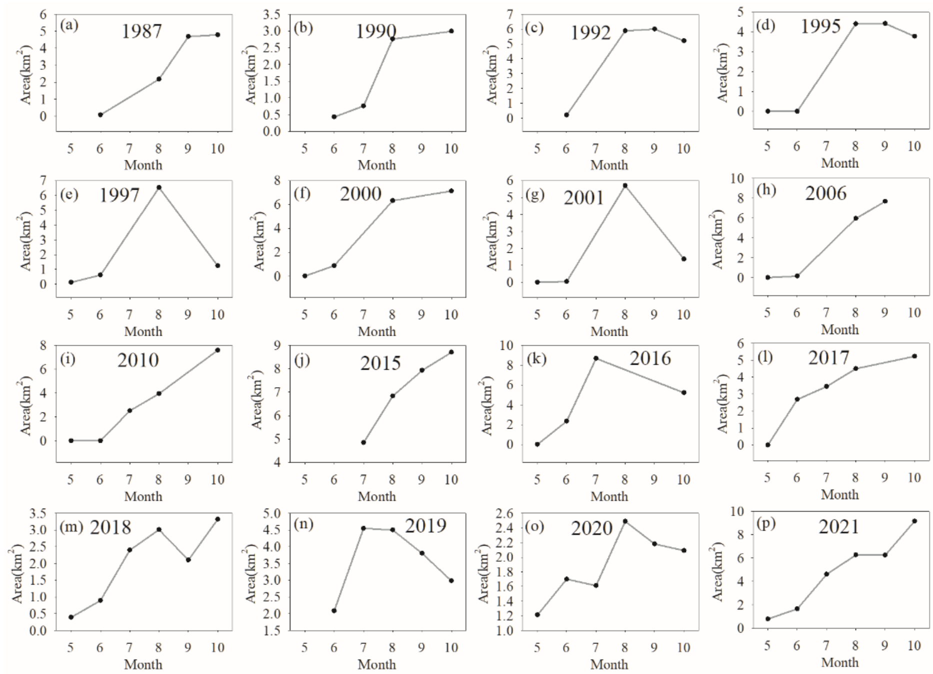

Figure 3. (**a**–**p**) Intra-annual variation patterns of FCBs in Qinghai Lake from 1987 to 2021.

3.1.2. Inter-Annual Change

Landsat TM/ETM+/OLI images from 1986 to 2017 and Sentinel-2 MSI images from 2016 to 2021 were used to analyze the long-term inter-annual variation characteristics of FCBs in Qinghai Lake. Due to the large variability of FCBs area between months, images from the same month were compared and analyzed from 1986 to 2021 for uniformity. Although there are no continuous year-by-year images for each month due to clouds, the available data can satisfy the need for analyzing change characterization over a long period. The numbers of images available in May, June, July, August, September and October are 17 (1989–2021), 25 (1986–2021), 16 (1990–2021), 20 (1987–2021), 16 (1987–2021) and 24 (1986–2021), respectively (Table 1).

Generally, the area of FCBs showed an increasing trend in all months, with the largest increase in July at 0.1 km^2/a, followed by October at 0.096 km^2/a, lesser increases in June, August and September, and smallest increase in May (Table 2 and Figure 4). The year 2004 was a turning point for water levels in Qinghai Lake, which stopped decreasing and started increasing, and a study shows that there is a correlation between FCBs area and the change in water levels in Qinghai Lake [11]. In this study, we used 2004 as a time point to segment and fit the area of FCBs of Qinghai Lake and analyze the area change trend before and after 2004. The results show that the area of FCBs in May and June was on a decreasing trend before 2004 and an increasing trend afterward. FCBs in July experienced an increasing trend for both pre- and post-2004 years, but the latter at a slightly lower rate than the former. Both August and October experienced an increase followed by a decrease, with the difference of that area change in October being more dramatic than in August. Changes before and after 2004 in September both showed a decreasing trend.

Specifically, FCBs were not monitored in May in most years, with smaller areas being recorded in 1989–1997 and essentially zero after 1997. After 2018, the area of FCBs increased, with a monitorable maximum value of 1.21 km^2 in 2020. The area of FCBs in June can be divided into three phases: a moderate amount of FCBs in 1986–2000, a relatively small area in 2000–2015 and a dramatic increase after 2015, with the largest area of 2.68 km^2 in 2017, followed by 2.34 km^2 in 2016 (Table 2 and Figure 4). The area of FCBs in July can be divided into two stages. With the dividing point of 2016, the FCBs showed a trend of increasing and then decreasing. The same trend was shown in August, with 2009 as the cut-off point. Both September and October can be divided into three phases, showing a fluctuating moderate area until 2005, a phase of consistently larger areas between 2005 and 2015, followed by a decrease and then a rebound in 2021. The maximum area of FCBs for September (8.67 km^2) and October (9.14 km^2) occurred in 2013 and 2021, respectively (Table 2).

Table 2. Change trends in the area of FCBs in Qinghai Lake from May to October, 1986–2021.

Month	Overall Change Rate (km^2/a)	Partitioned Change Trend (km^2/a)		Largest Area	
		Before 2004	After 2004	km^2	Year
May	0.013	−0.011	0.050	1.21	2020
June	0.028	−0.011	0.141	2.67	2017
July	0.100	0.132	0.108	8.67	2016
August	0.023	0.200	−0.169	8.75	2009
September	0.020	−0.082	−0.052	8.67	2013
October	0.096	0.025	−0.396	9.14	2021

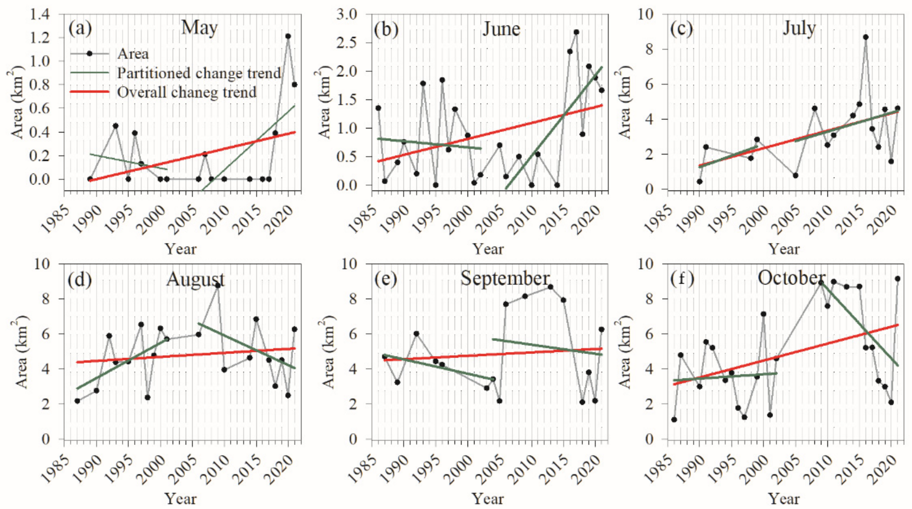

Figure 4. (**a**–**f**) Inter-annual variation of peak FCBs area in Qinghai Lake from 1986 to 2021.

3.2. Spatial Pattern

3.2.1. Spatial Distribution

FCBs in Qinghai Lake are mainly distributed in the SR, SRB, QR, BRN, BRS, QB and HR regions (Figure 1b). The distribution of FCBs is uneven among regions, and the average value of the area in each region as a percentage of the total area in Qinghai Lake from 1986 to 2021 shows that the area of FCBs in seven regions, in descending order, was: BRN region (35.32%), QB (17.90%), BRS region (16.94%), SRB region (11.32%), SR region (7.41%), HR region (5.56%) and QR region (5.55%). However, FCBs in each region had different change patterns.

3.2.2. Spatial Change Pattern

Based on the maximum area of FCBs of each year in Qinghai Lake from 1986 to 2021, the inter-annual variation characteristics of FCBs in seven main distributed areas were analyzed. Overall, the area of FCBs in BRN and BRS regions showed an obvious and dramatic increasing trend; the area percent share also had a gradually increasing trend. The RBN region experienced the most dramatic growth, with the increasing rates of area and area percent of 0.06 km^2/a and 0.65 %/a, respectively. Since 2009, the BRN region has been frequently covered by FCBs larger than 2 km^2, which was at a high value of 4.67 km^2 in 2021, covering more than half of the total FCBs area in Qinghai Lake (51.07%) (Table 3, Figures 5–7). The BRS region suffered the second largest increase in FCBs, with the area and area percent increasing rates of 0.03 km^2/a and 0.38%/a. The year 2021 was also one with the largest FCBs area during the study period, which was 2.44 km^2, accounting for

26.64% of the total area of Qinghai Lake. The area of FCBs in the SRB, SR and QB regions showed a very weak increasing trend of less than 0.01 km^2/a, and the area percent of FCBs in the SR region also had a very slight increase (0.03%/a). Meanwhile, the area percent in the SRB and QB regions presented a decreasing trend, with a decreasing rate of −0.21 %/a and −0.41 %/a (Table 3). The area and area percent of FCBs in QR and HR regions both had a significant reduction trend, with a decreasing area rate of −0.007 km^2/a and the area percent decreasing rates of −0.19 %/a and −0.26 %/a, respectively. It is noteworthy that the area of FCBs in SR, QR, QB and HR regions all had a significant decrease in the last 5 years (Figure 5).

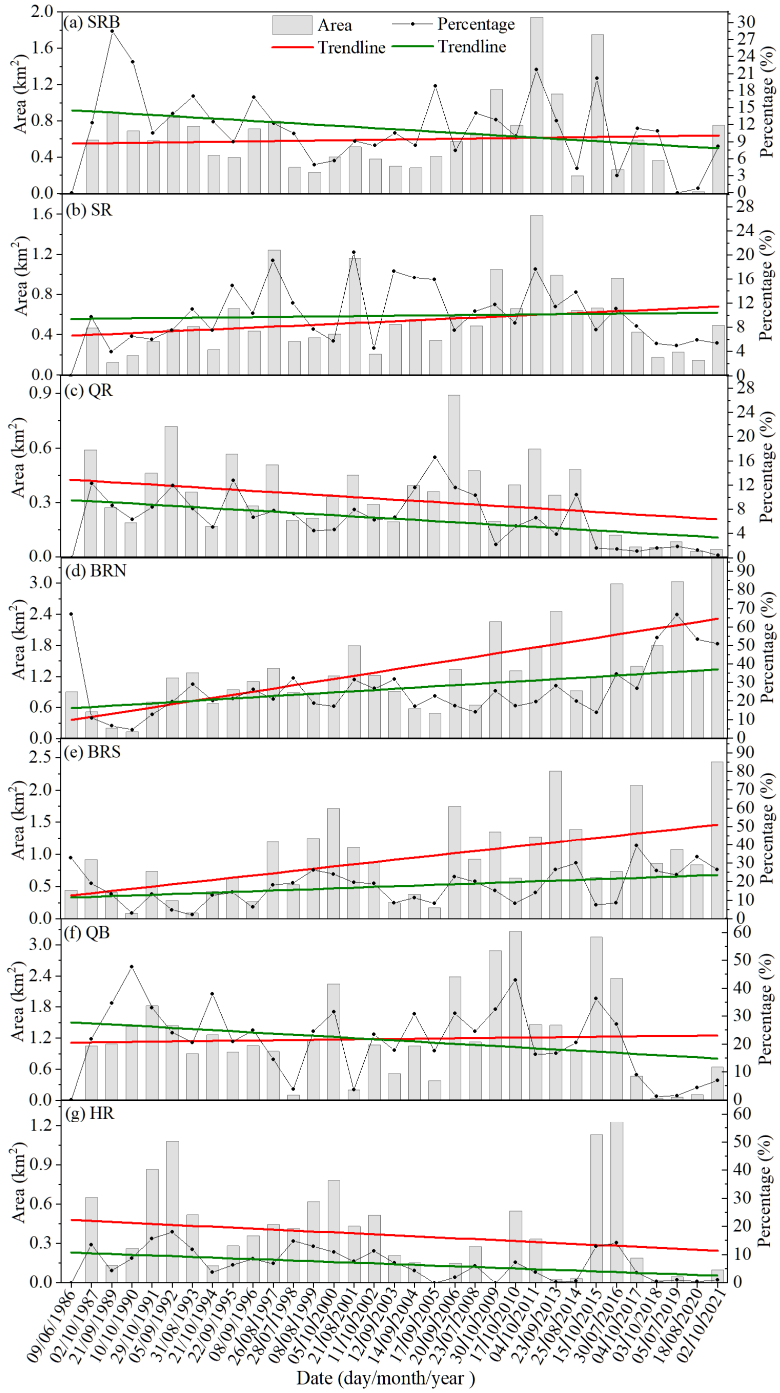

Figure 5. (**a**–**g**) Intra-annual variation characteristics of FCBs in each region of Qinghai Lake from 1986–2021.

Table 3. Change trends in the area of FCBs indifferent regions of Qinghai Lake from 1986 to 2021.

	SRB	SR	QR	BRN	BRS	QB	HR
Area (km^2/a)	0.003	0.009	−0.007	0.06	0.03	0.004	−0.007
Area percent (%/a)	−0.21	0.03	−0.19	0.65	0.38	−0.41	−0.26

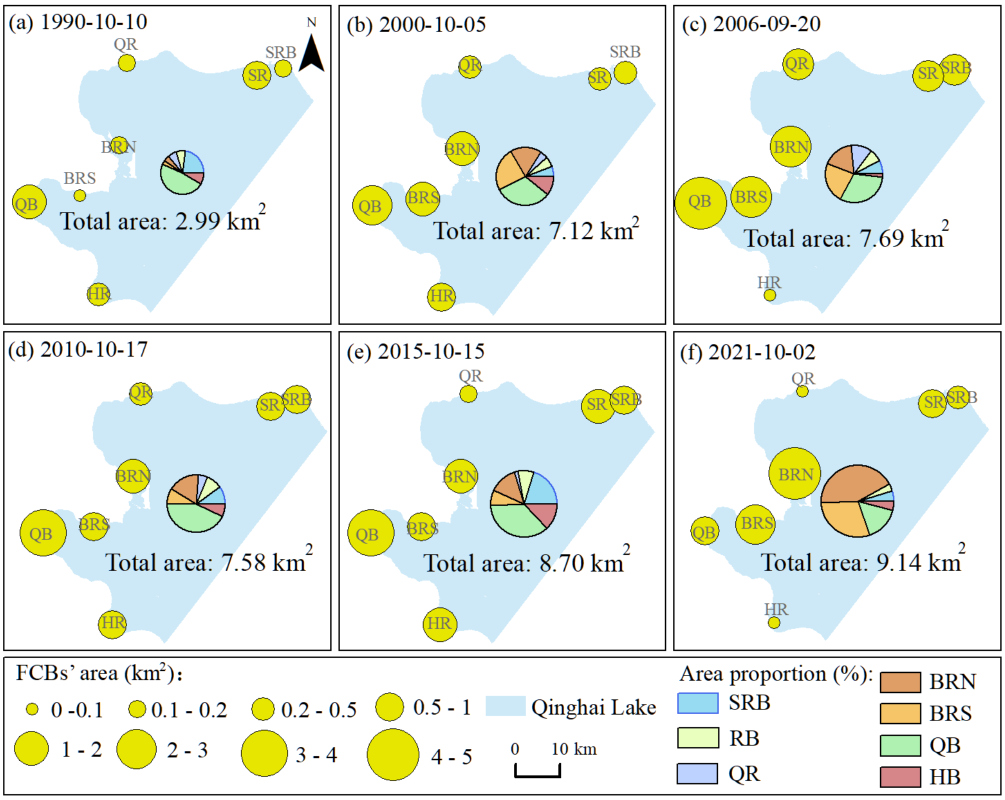

Figure 6. (**a**–**f**) Area and its proportion of FCBs in different regions of Qinghai Lake for 1990, 2000, 2006, 2010, 2015 and 2021.

The spatial distribution of the maximum FCBs area in 1990, 2000, 2005, 2010, 2015 and 2021 showed that in 1990, most FCBs in Qinghai Lake were distributed in the QB region, accounting for 52.25% of the total area in Qinghai Lake, followed by the SR region. In 2000 and 2005, the largest FCBs area was also in the QB region, followed by the BRS and BRN regions. In 2010 and 2015, it still showed the QB region as the largest area, followed by the BRN region and SRB region. In 2021, the BRN region had the largest area of FCBs, followed by the BRS region and SRB region. It can be seen from the time axis that the BRN region has gradually become the region with the most concentrated distribution of FCBs in Qinghai Lake (Figures 6 and 7). In addition, because algal blooms are usually distributed on the shore, the water bloom of Qinghai Lake undergoes a spatial change process from outward to inward, and again to outward of water body, as water levels of Qinghai Lake grow, which can be clearly presented in Figure 7.

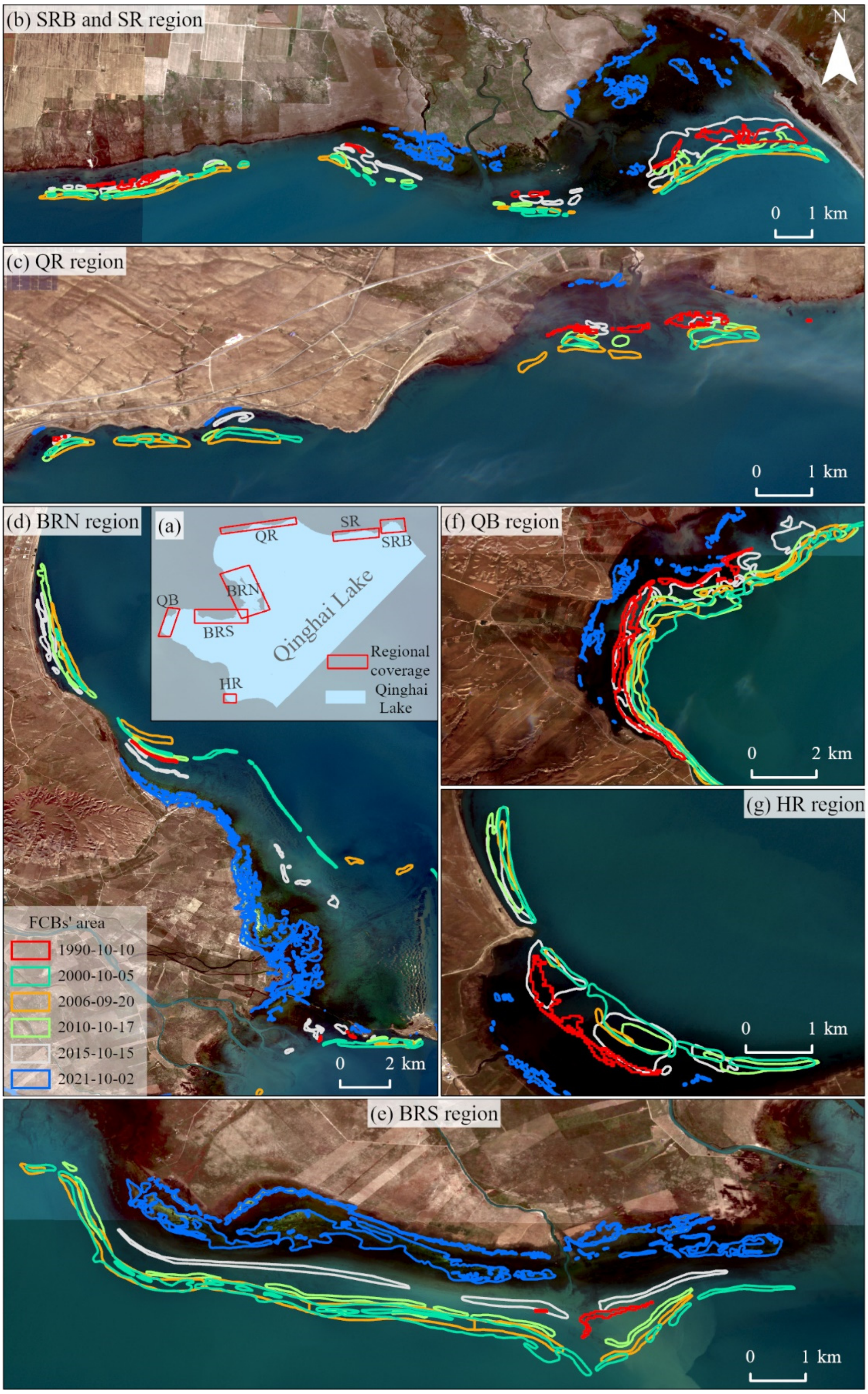

Figure 7. (**a**–**g**) Spatial evolution patterns of FCBs in each region of Qinghai Lake from 1986–2021 (Background: Sentinel-2 MSI image Band composition: 4-3-2, Date: 2 October 2021).

4. Discussion

4.1. Accuracy and Consistency Evaluation

In this study, the long-term change characteristic of FCBs in Qinghai Lake was analyzed based on multi-source remote sensing images of Landsat TM/ETM+/OLI and Sentinel-2 MSI images, for which it is essential to verify the accuracy of the FCBs area extracted by FAI method. The validation of classification accuracy for remote sensing images is usually achieved by field data or higher-resolution images. In this study, the manually digitalized FCBs areas from UAV images were used as the true value to evaluate the FAI-extracted results. Acquiring UAV images with the same date as the satellite remote sensing images is a less easy task to achieve, but the UAV image covering the Bird Island region (included in the BRN region) we acquired on 6 September 2019 is only three days away from the Sentinel-2 image taken on 3 September, and the UAV image taken on 23 July 2021 is only four days away from the Landsat ETM+ image taken on July 19. Although the biomass of algal blooms can change greatly in a short period of time [43], the blooms are subject to wind blowing and accumulate in strips on the shore, maintaining a relatively stable area, so the quasi-synchronous UAV images can also be used as true values to verify the accuracy of the results extracted from the satellite remote sensing images by the FAI method. For Landsat ETM+ images, we extracted FCBs using FAI method by the initial 30 m spatial resolution images and the 15 m spatial resolution images after pan-sharpened process, where the former can represent the area of FCBs extracted based on Landsat TM images, and the latter represents the area of FCBs extracted based on Landsat ETM+/OLI images.

The result shows that FCBs area visually interpreted by UAV imagery on 23 July 2021 was 0.99 km^2 and that the areas extracted from Landsat ETM+ image with spatial resolution of 30 m and 15 m were 1.19 km^2 and 1.09 km^2, respectively. Therefore, the area error from the images with spatial resolution of 30 m is 20.2%; it is 10.2% for images of 15 m spatial resolution (Figure 10a,b). Meanwhile, the area of FCBs visually interpreted from UAV images on 6 September 2019 was 0.41 km^2; when extracted from Sentinel-2 MSI images on 3 September 2019, the area was 0.45 km^2, resulting in area error of 9.76% (Figure 8c,d). The accuracy evaluation shows that images with lower spatial resolution obtained larger FCBs area, causing a larger error. That may be due to the inclusion of more non-algae parts in a larger spatial resolution pixel. In addition, the UAV images are not fully synchronized with Landsat ETM+ and Sentinel-2 MSI images. There is a time difference of 3–4 days, which is not enough for the FCBs to change on a large scale; however, some area change could occur and thus increase the area error.

Furthermore, different remote sensing images have different spatial resolutions, which results in different extracted areas of FCBs. Comparing the area of FCBs from the same day based on different data sources, the area difference can be explored and illustrated. Fortunately, a scene of Landsat OLI image and a scene of Sentinel-2 MSI image from 28 August 2021 are both available. Based on Landsat OLI images, the FCBs area can be extracted from images with both 30 m and 15 m spatial resolution. The former (30 m) was used to represent the area of FCBs extracted from Landsat TM images, and the latter (15 m) was used to represent the area extracted from Landsat ETM+ and OLI images. Additionally, then, the FCB's area extracted based on two different spatial resolutions (30 m and 15 m) was compared with that extracted based on Sentinel-2 MSI images (10 m), which were used to illustrate the area differences of FCBs extracted from different sources of images.

The results show that on 28 August 2021, the areas of FCBs in Bird Island region extracted from images with spatial resolution of 10 m, 15 m and 30 m were 1.34 km^2, 1.36 km^2 and 1.41 km^2, respectively (Figure 9). The areas of FCBs extracted from images with spatial resolution of 10 m were 1.49% and 5.22% smaller than those from images with spatial resolution of 15 m and 30 m, respectively. The same conclusion was drawn, namely that the lower the spatial resolution of the image, the larger the area of the extracted FCBs obtained. That is, the area of FCBs extracted based on Landsat TM images from 1986 to 2011 is overestimated. It also indicates that the increase in FCBs should have been more dramatic over the past 36 years.

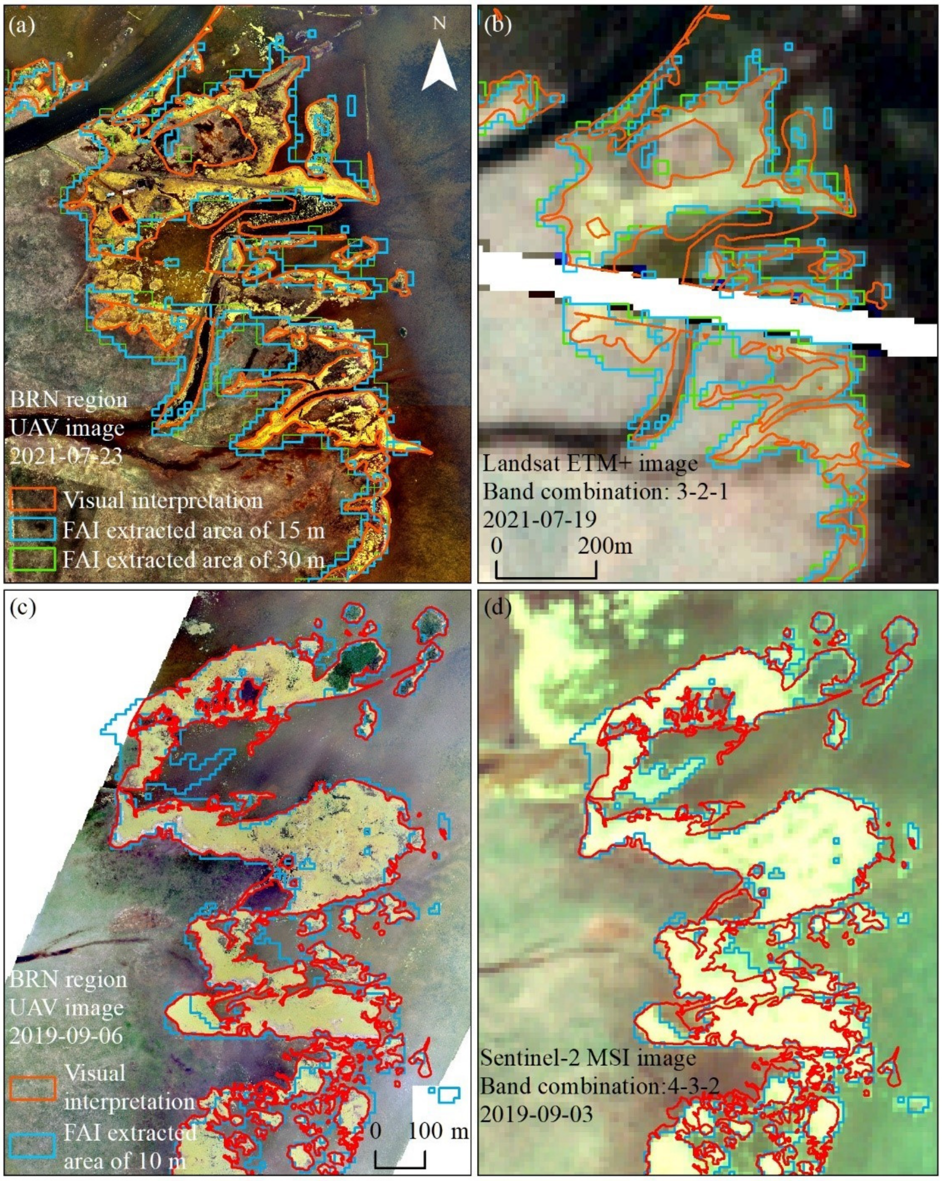

Figure 8. Accuracy evaluation of the FAI method-extracted FCBs area from Landsat TM/ETM+/OLI and Sentinel-2 MSI images. (**a**) and (**b**) UAV image taken on 23 July 2021 used to validate the FAI result from Landsat ETM+ images (15 m and 30 m) taken on 19 July 2021; (**c**) and (**d**) UAV image taken on 6 September 2019 used to validate the FAI-result from Sentinel-2 MSI image (10 m) taken on 3 September 2019.

4.2. Driving Forces

Investigating the driving factors for the large appearance of FCBs in Qinghai Lake is an important prerequisite for its control and management. Research shows that the stable substrate, abundant nutrient, sufficient sunlight and suitable temperature are favorable conditions for the growth of Cladophora in Qinghai Lake [11,44]. Since 2004, the Qinghai Lake has continued to rise and expand, inundating large areas of land along its shores [35], in which the western and northern regions are mainly covered by pastures. Therefore, the undecomposed plant residues in the submerged pastures in the western region serve as a good adhesion substrate for Cladophora. In addition, although the overall nutrient salinity of Qinghai Lake remains stable [10], some localized areas may have high nutrient salt content induced by the large amounts of droppings from cattle, sheep and birds, promoting the growth of Cladophora.

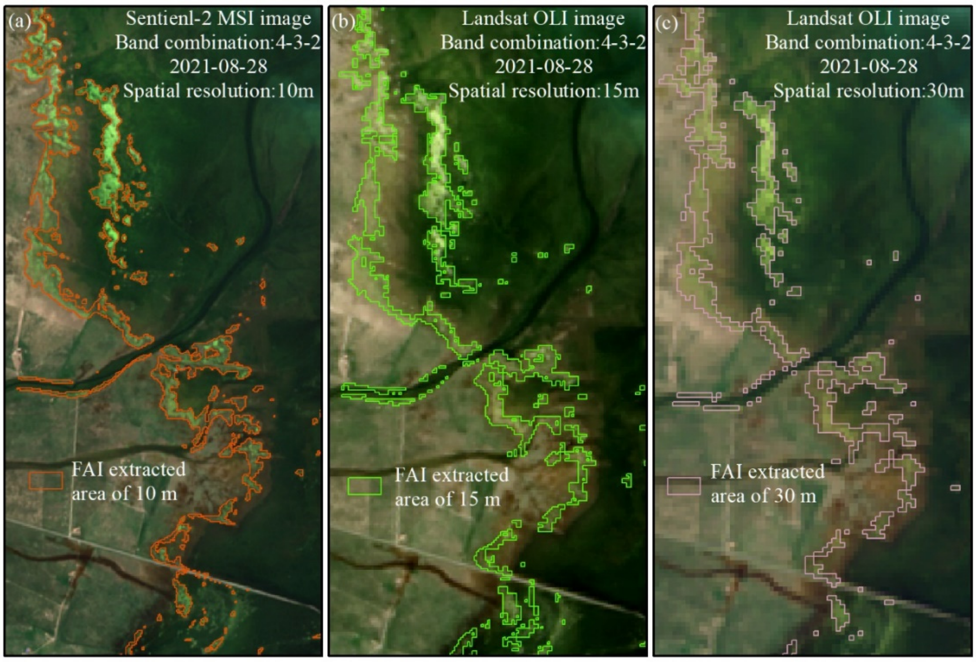

Figure 9. Illustration of area difference for FCBs extracted from different images (**a**) from Sentinel-2 MSI image with spatial resolution of 10 m, (**b**) from Landsat OLI image with spatial resolution of 15 m and (**c**) from Landsat OLI image with spatial resolution of 30 m.

The intra-annual variation of FCBs in Qinghai Lake showed a characteristic of starting in May, increasing rapidly from June to August, and increasing slowly from September to October in most years (1987, 1990, 2000, 2006, 2010, 2015, 2017, 2018, 2019 and 2021). Thereafter, these years were named group 1, for which the maximum area of FCBs occurred in October. Another common situation is that, after a rapid increase in FCBs from June to August, the area decreased in September and October, with the maximum value in July or August (1992, 1995, 1997, 2001, 2016, 2019 and 2020). These years are named as group 2. The comparison shows that group 1 had relatively warmer temperatures than group 2 in July (0.96 °C) and October (0.37 °C), but slightly colder temperatures in July (0.15 °C) and September (0.03 °C) (Table 5). Group 1 had 0.41 h and 0.01 h more sunshine than group 2 in July and August, respectively, while they had 0.39 h and 0.1 h less sunshine than group 2 in September and October, respectively. The optimum temperature range for the growth of Cladophora is 15–20 °C [44], therefore, the best season for the growth of Cladophora in Qinghai Lake is July and August (Table 4). However, the peak area of FCBs in Qinghai Lake occurred in September or October in most years (group 1), or August in fewer years (group 2). This may be related to the morphology of Cladophora in Qinghai Lake, which exist in two forms: the attaching type and the floating type [11]. The latter appears only when the former reaches a certain biomass and can be captured clearly by remote sensing images, which is the objective in this paper. A certain time interval exists between the massive growth of attached Cladophora and the generation of floating blooms. Therefore, we speculate that it may be a reason for the different appearance time of the maximum FCBs area in different years. Group 1 had high temperatures in July, which favored the growth of large amounts of attached Cladophora, but had a relatively low temperature in August, which hinders the conversion process of attached Cladophora to floating Cladophora blooms. Additionally, then, the relatively high temperatures in October again promoted the formation of large scales of floating blooms (Table 4). Contrary to group 1, group 2 experienced relatively low temperatures in July, resulting in a relatively smaller accumulation of Cladophora; higher temperatures in August promoted the conversion of floating Cladophora blooms, and lower temperatures in October resulted in a smaller area of FCBs. In addition, it has been shown that the growth of Cladophora in the northern temperate zone follows a bi-seasonal pattern: a brief peak in biomass occurs in the summer [45], after which biomass decreases, and the second biomass peak occurs in the autumn [46–48]. This may be the reason why the FCBs reach their peak in September and October in most of the years.

Table 4. The mean temperature, mean sunshine hours and mean windspeed for two groups of years from July to October.

Group	July			August			September			October		
	T (°C)	SH (h)	WS (m/s)	T (°C)	SH (h)	WS (m/s)	T (°C)	SH (h)	WS (m/s)	T (°C)	SH (h)	WS (m/s)
1	18.22	8.18	3.11	17.04	7.74	2.89	13.25	7.16	2.81	8.58	8.21	2.85
2	17.26	7.77	3.14	17.19	7.73	3.03	13.28	7.55	2.86	8.21	8.23	2.95
Total	17.80	8.00	3.12	17.11	7.74	2.95	13.26	7.33	2.83	8.42	8.22	2.89

Note: T, SH and WS refers to Temperature, Sunshine and Windspeed. Group 1 includes years (1987, 1990, 2000, 2006, 2010, 2015, 2017, 2018, 2019 and 2021) featuring the maximum annual FCBs in September and October. Group 2 includes years (1987, 1990, 2000, 2006, 2010, 2015, 2017, 2018, 2019 and 2021) featuring the maximum annual FCBs in July and August (1992, 1995, 1997, 2001, 2016, 2019 and 2020).

From 1986 to 2021, the annual maximum area of FCBs in Qinghai Lake has had a significant increasing trend. A study shows that algal blooms are positively correlated with temperature and sunshine, and negatively correlated with wind speed and precipitation [49]. In this study, we analyzed the correlation between FCBs area and mean maximum temperature, mean sunshine hours, mean wind speed and mean precipitation for each month, from May to October in 1986–2015. The results demonstrate that there has been very weak or no correlation between FCBs area and temperature, sunshine, wind speed and precipitation in each month (Table 5 and Figure 10). The impact of sunshine on Cladophora is that sufficient sunshine promotes growth, but strong sunshine is detrimental to Cladophora [38]. In May, the FCBs area was negatively correlated with sunshine hours. However, this may have been caused by serendipity because sunshine is not strong in May in Qinghai Lake, and Cladophora starts to grow in May, when adequate light is a better. Additionally, the FCBs area was negatively correlated with wind speed in June and October ($p < 0.1$) (Table 5), which is in line with previous study, which illustrates that faster wind speed can cause algal bloom particles to sink underwater, reducing the concentration [13]. Cambridge deemed that 15–20 °C is the most suitable temperature range for Cladophora [44], however, other studies also show that different species of Cladophora in different lakes have different temperature responses [38]. None of the months in this study shows a correlation between FCBs area and temperature. However, in some months of some years, larger scale of FCBs corresponded to the relatively higher temperatures, such as June in 2016 and 2021, September in 2009 and 2021, and October in 1991, 2000, 2010 and 2021 (Figure 10). Precipitation can reduce the FCBs by reducing the temperature of water surface and the concentration of nutrients. However, we did not derive a significant correlation between FCBs area and precipitation in Qinghai Lake in this study.

Table 5. Correlation of FCBs area with monthly average of maximum temperature, monthly average of sunshine hours and monthly average of mean windspeed for May to October, 1986 to 2021.

Month	Temperature		Sunshine Hours		Wind Speed		Precipitation	
	R	P	R	P	R	P	R	P
May	−0.05	0.85	−0.513 *	0.035	−0.157	0.548	0.3729	0.1405
June	−0.117	0.577	−0.362	0.076	−0.469 *	0.018	0.0502	0.8117
July	0.231	0.39	0.15	0.578	−0.397	0.128	0.4183	0.1067
August	−0.118	0.620	−0.135	0.571	−0.071	0.766	0.3025	0.1949
September	−0.108	0.69	−0.123	0.651	0.104	0.581	0.0971	0.7204
October	0.164	0.445	−0.0333	0.112	−0.456 *	0.025	0.2835	0.1795

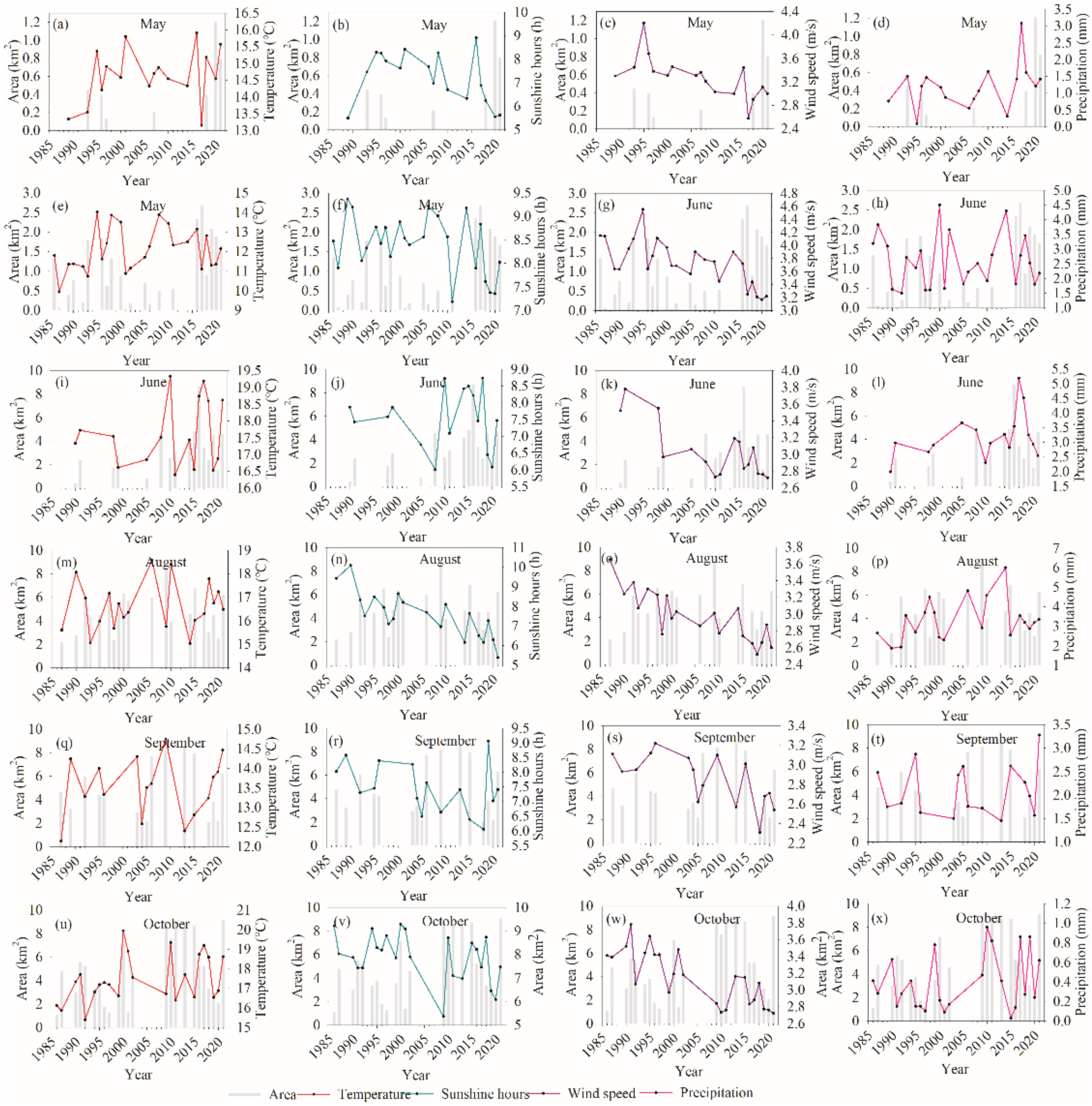

Figure 10. (**a**–**x**) Illustration of FCBs area with corresponding monthly average of maximum temperature, monthly average of sunshine hours and monthly average of mean windspeed for May to October, 1986 to 2021.

Currently, the quantitative study of the mechanism for large scale FCBs is difficult due to a lack of specific quantitative research on the suitable growth environment for Cladophora in Qinghai Lake because: (1) the available images for extracting FCBs are limited, especially before 2015, which hinders the understanding of more specific patterns of FCBs change; (2) there is an optimal range for algal blooms growth in terms of temperature and sunlight—too high or too low is not conducive to the growth of algal blooms, but this range for Cladophora in Qinghai Lake is unknown; (3) Cladophora is influenced by factors other than meteorological ones, which are complicated, scarce and difficult to clarify.

FCBs in Qinghai Lake are mainly distributed in each estuary and lake bay regions on the west and north sides. Over the past 36 years, FCBs area has shown a significant increasing trend in the BRN and BRS regions, a slight increase in the SR region and a decreasing trend in the QR region and HR region. The increase in FCBs area in the BRN and BRS regions can be attributed to a large amount of inundated grassland, which provides a richer attachment substrate and nutrients; this is a reasonable and accepted explanation [11,43]. The SRB and SR regions have also had a large outward expansion, while the area of FCBs was largely stable. Unlike other regions of Qinghai Lake, the inundated land here includes dry farmland, herbaceous plants and coniferous forests, in addition to grassland, which may influence the growth of Cladophora to some extent, but this is not currently clear. The QR region has expanded less outward, which should be due to the relatively steep terrain and thus resulting in deeper water, reducing the sunshine for Cladophora. Therefore, the FCBs in the QR region experienced a decreasing trend, especially after 2015, when there were very little amounts of FCBs. Until 2016, the QB region had been the main distribution area of FCBs in Qinghai Lake (Figures 5 and 6), but since 2017, the FCBs area has shrunk, although the water body has still largely expanded outward, and the cause is not yet known. The HR region had a large variable FCBs, with the largest area in 2015 and 2016, but since 2017, there has been essentially no monitorable FCBs despite the large scale of inundated grassland, and the cause of this is currently unknown.

In recent years, the ecological protection of Qinghai Lake has received widespread attention, and then the problem of Cladophora blooms in Qinghai Lake also became a hot issue of concern. The Qinghai Lake National Nature Reserve Administration took measures to control the Cladophora blooms by manually salvaging the FCBs and cleaning up the animal manure in regions with heavy blooms (Bird Island region), which can inhibit FCBs to a certain extent. The maximum area of FCBs in 2016 was 8.67 km^2; then it decreased in 2017, 2018, 2019 and 2020, with the areas of 5.22 km^2, 3.32 km^2, 4.55 km^2 and 2.49 km^2, respectively. However, the maximum area reached up to 9.14 km^2 in 2021. This may be because the salvage work was mainly carried out in 2017–2020, and the large FCBs appeared again in 2021 when no manual control work was implemented. It can be seen that artificial salvaging of FCBs is a symptomatic but not a curative measure. However, at present, it has had a better effect on FCBs control. After that, more fundamental measures should be studied.

5. Conclusions

In this study, a total of 118 periods of data on FCBs area was extracted based on Landsat TM/ETM+/OLI images from 1986 to 2017 and Sentinel-2 MSI images from 2016 to 2021, using the FAI method to study the spatial change and temporal patterns of FCBs in Qinghai Lake. We intended to provide a comprehensive analysis of the long-term area changes of Cladophora blooms in Qinghai Lake and to provide data support and theoretical references for the government and other studies related to the ecological environment of Qinghai Lake. The main conclusions are as follows:

1. The area of FCBs in Qinghai Lake from May to October showed a general change trend of starting in May, expanding rapidly from June to August and increasing steadily from September to October, and in fewer years, the FCBs peaked in July or August. From 1986 to 2021, the area of FCBs in Qinghai Lake showed an overall increasing trend in all months, with the largest increase in July at 0.1 km^2/a, followed by October at 0.096 km^2/a. In particular, each month showed different stages of change, with May and June showing a decrease followed by an increase, July showing a consistent increase, August showing an increase followed by a decrease, and September and October showing a decrease followed by an increase and then a decrease.
2. FCBs in Qinghai Lake are mainly distributed in each estuary and lake bay regions on the west and north sides. Over the past 36 years, FCBs area showed a significant increasing trend in the BRN and BRS regions, a slight increase in the SR region and a decreasing trend in the QR region and the HR region.
3. Studies of the driving forces of FCBs changes show that the intra-annual variation of FCBs may be due, firstly, to the presence of two types of morphology of Cladophora, attached and floating, and the transformation between the two types takes some time. Second, differences in temperature and light in different months lead to temporal differences in the biomass and morphological transformation of FCBs. The third is the potential influence of the double biomass peak pattern of algae in the northern

hemisphere. The correlation between FCBs and meteorological elements was weak or largely uncorrelated, which may also be due to the small sample size. However, the negative correlation between wind speed and algal bloom was manifested in June and October.

4. The inundated land caused by rising water levels in Qinghai Lake provided a large amount of substrate for Cladophora to adhere to, which, together with the shallow water environment in the inundated area favoring sunlight and the nutrients released from bird and animal excreta, led to a significant increase in FCBs area in the BRN region, which has become the largest area of FCBs in Qinghai Lake. The salvage measures for FCBs in this region by the Qinghai Lake management agencies showed their effectiveness in controlling the FCBs, resulting in the reduction of FCBs area in 2017–2020. However, more essential governance measures should be explored afterward.

Author Contributions: Conceptualization, H.D. and X.Y.; methodology, H.D.; software, H.D.; validation, X.Y., Q.W. and D.Z.; formal analysis, D.Z.; investigation, H.J.; resources, H.J.; data curation, Q.W.; writing—original draft preparation, H.D.; writing—review and editing, X.Y.; visualization, H.D.; supervision, X.Y.; project administration, X.Y.; funding acquisition, X.Y. All authors have read and agreed to the published version of the manuscript.

Funding: This research was jointly funded by the Natural Science Foundation of China (no. 41861013; no. 42071089), Longyuan Youth Innovation and Entrepreneurship Program of Gansu Province and Chinese Academy of Sciences "Light of West China" Program, the "Innovation Star" of Outstanding Graduate Student Program in Gansu Province (2021-CXZX-215), Northwest Normal University's 2020 Graduate Research Grant Program (2020KYZZ001012).

Data Availability Statement: No applicable.

Acknowledgments: The authors would like to thank staff in Qinghai Lake Nature Reserve Administration for great help in conducting field work.

Conflicts of Interest: The authors declare no conflict of interest. The funders had no role in the design of the study; in the collection, analyses, or interpretation of data; in the writing of the manuscript, or in the decision to publish the results.

References

1. Cao, M.; Song, Q.; Jin, E.; Hao, Y.; Zhao, W. A spectral index for the detection of algal blooms using Sentinel-2 Multispectral Instrument (MSI) imagery: A case study of Hulun Lake, China. *Int. J. Remote Sens.* **2021**, *42*, 4514–4535. [CrossRef]
2. Lai, L.; Zhang, Y.; Jing, Y.; Liu, Z. Research progress on remote sensing monitoring of phytoplankton in eutrophic water. *J. Lake Sci.* **2021**, *33*, 1299–1314. [CrossRef]
3. Ho, J.; Michalak, A.; Pahlevan, N. Widespread global increase in intense lake phytoplankton blooms since the 1980s. *Nature* **2019**, *574*, 667–670. [CrossRef] [PubMed]
4. Susan, B.; Watson, A.; Carol, M.; George, A.; Gregory, L.; Wayne, C.; Murray, N.; Charlton, F.; Remegio, C.; David, C.; et al. The re-eutrophication of Lake Erie: Harmful algal blooms and hypoxia. *Harmful Algae* **2016**, *56*, 44–66.
5. Ulrich, A.; Malley, D.; Watts, P. Lake Winnipeg Basin: Advocacy, challenges and progress for sustainable phosphorus and eutrophication control. *Sci. Total Environ.* **2015**, *542*, 1030–1039. [CrossRef]
6. Qin, B.; Deng, J.; Paerl, H.; Brookes, J.; Liu, J.; Jeppesen, E.; Zhu, G.; Zhang, Y.; Xu, H.; Shi, K. Why Lake Taihu continues to be plagued with cyanobacterial blooms through 10 years (2007–2017) efforts. *Sci. Bull.* **2019**, *64*, 7–9. [CrossRef]
7. Huang, J.; Zhang, Y.; Huang, Q.; Gao, J. When and where to reduce nutrient for controlling harmful algal blooms in large eutrophic lake Chaohu, China? *Ecol. Indic. Integr. Monit. Assess. Manag.* **2018**, *89*, 808–817. [CrossRef]
8. Wu, Z.; Liu, Y.; Liang, Z.; Wu, S.; Guo, H. Internal cycling, not external loading, decides the nutrient limitation in eutrophic lake: A dynamic model with temporal Bayesian hierarchical inference. *Water Res.* **2017**, *116*, 231–240. [CrossRef]
9. Wu, Q.; Xie, P.; Yang, L.; Gao, G.; Liu, Z.; Pan, G.; Zhu, Z. Ecological consequences of cyanobacetrial blooms in lakes and their countermeasures. *Adv. Earth Sci.* **2008**, *23*, 1115–1123.
10. Guo, L.; Li, L.; Li, L.; Li, G. The characteristics of Cladophora community and its influencing factors in a eutrophic lake. *China Environ. Sci.* **2017**, *37*, 4667–4674.
11. Hao, M.; Zhu, H.; Xiong, X.; He, Y.; Ao, H.; Yu, G.; Wu, C.; Liu, G.; Luo, Z.; Liu, J. Analysis on the distribution and origin of Cladophora in the nearshore water of Qinghai Lake. *Acta Hydrobiol. Sin.* **2020**, *44*, 1152–1158.
12. Jia, T.; Zhang, X.; Dong, R. Long-term spatial and temporal monitoring of Cyanobacteria blooms using MODIS on Google Earth Engine: A Case Study in Taihu Lake. *Remote Sens.* **2019**, *11*, 2269. [CrossRef]

13. Ma, J.; Jin, S.; Li, J.; He, Y.; Shang, W. Spatio-temporal variations and driving forces of harmful algal blooms in Chaohu Lake: A multi-source remote sensing approach. *Remote Sens.* **2021**, *13*, 427. [CrossRef]
14. Li, S.; Liu, J.; Song, K.; Liang, C.; Gao, J. Analysis on spatial and temporal character of Cladophora blooms in lake Chaohu and its driving factors based on Landsat imagery. *Resour. Environ. Yangtze Basin* **2021**, *28*, 1205–1213.
15. Li, Y.; Shi, Z.; Zhang, Y.; Zhao, Q.; Li, A.; Jin, Y.; Tie, C. Evaluation method and application on Cyanobacteria bloom degree classification with algal density. *Environ. Sustain. Dev.* **2014**, *39*, 67–68.
16. Li, L.; Li, G.; Li, G. Winter and spring succession of the Phytoplankton community in Dianchi Lake under the influences of environment change. *J. Hydroecol.* **2020**, *41*, 57–68.
17. Zheng, W.; Han, X.; Liu, C.; Li, Y. Satellite remote sensing data monitoring "Huang Tai" Cladophora blooms in Lake Ulansuhai, lnner Mongolia. *J. Lake Sci.* **2010**, *22*, 321–326.
18. Wang, Y.; Huang, Y.; Yu, C.; Qi, Y.; Zhang, J. Detection of temporal and spatial variation of Huangtai Cladophora blooms using MODlS satellite data in Lake Ulansuhai from 2000 to 2010. *J. Lake Sci.* **2012**, *24*, 519–527.
19. Yue, A.; Ji, Y.; Liu, H.; Zhang, Z. Historical regional distribution specialties of algal bloom extraction from Yuqiao Reservoir via Landsat 8 and its driving factors. *J. Saf. Environ.* **2019**, *19*, 1448–1455.
20. Zhang, Y. Eutrophication Study for Yuqiao Reservoir. Master's Thesis, Tianjin University, Tianjin, China, 2011.
21. Chen, J.; Wang, J.; Wang, Q.; Lv, J.; Li, N. Common fate of sister lakes in Hulunbuir Grassland: Long-term harmful algal bloom crisis from multi-source remote sensing insights. *J. Hydrol.* **2021**, *594*, 125970. [CrossRef]
22. Li, S. A preliminary study on the types, evolution and biological productivity of Qinghai Lake. In Proceedings of the Second Plenary Session of the Western Pacific Fisheries Research Commission; Science Press: Beijing, China, 1959; pp. 97–105.
23. Lanzhou Institute of Geology. *Comprehensive Investigation Report of Qinghai Lake*; Science Press: Beijing, China, 1979; pp. 15–22.
24. Yang, H.; Wang, J. Analysis on the benthos and their productivity in Qinghai Lake. *Qinghai Sci. Technol.* **1997**, *4*, 36–39.
25. Yao, W.; Shi, J.; Qi, H.; Yang, J.; Jia, L.; Pu, J. Study on the phytoplankton in Qinghai Lake during the summer of 2006–2100. *Freshw. Fish.* **2011**, *41*, 22–28.
26. Zhao, Z.; Zhu, H.; Xiong, X.; He, Y.; Ao, H.; Wu, C. The identification of Cladophora Qinghaiensis SP. Nov., within the genus Cladophora collected from Qinghai Lake, China. *Acta Hydrobiol. Sin.* **2021**, *45*, 663–669.
27. Wen, X.; Jing, Y.; Zhang, D. Review on application of common satellite sensors in monitoring algal blooms. *Environ. Sci. Technol.* **2014**, *37*, 81–87.
28. Duan, H.; Zhang, S.; Zhang, Y. Cyanobacteria bloom monitoring with remote sensing in Lake Taihu. *J. Lake Sci.* **2008**, *20*, 145–152.
29. Ma, R.; Kong, F.; Duan, H.; Zhang, S.; Kong, W.; Hao, J. Spatio-temporal distribution of cyanobacteria blooms based on satellite imageries in Lake Taihu, China. *J. Lake Sci.* **2008**, *20*, 687–694.
30. Xu, J.; Zhang, B.; Li, F.; Song, K.; Wang, Z. Detecting modes of cyanobacteria bloom using MODIS data in Lake Taihu. *J. Lake Sci.* **2008**, *20*, 191–195.
31. Hu, C. A novel ocean color index to detect floating algae in the global oceans. *Remote Sens. Environ.* **2009**, *113*, 2118–2129. [CrossRef]
32. Guo, W. Study on Extraction methods of cyanophytes bloom based on HJ-1. Master's Thesis, Nanjing Normal University, Nanjing, China, 2011.
33. Matthews, M.; Odermatt, D. Improved algorithm for routine monitoring of cyanobacteria and eutrophication in inland and near-coastal waters. *Remote Sens. Environ.* **2015**, *156*, 374–382. [CrossRef]
34. Li, X.; Zhang, Y.; Shi, H.; Jiang, S.; Wang, T.; Ding, M.; Cai, K. Application of Maximum Chlorophyl Index derived from Sentinel-3A satellite OLCI data for monitoring Cyanobacteria blooms in lake Taihu. *Environ. Monit. China* **2019**, *35*, 146–155.
35. Qi, M.; Yao, X.; Liu, S.; Zhu, Y.; Gao, Y.; Liu, B. Dynamic change of Lake Qinghai shoreline from 1973 to 2018. *J. Lake Sci.* **2020**, *32*, 573–583.
36. Du, J.; Li, Q.; Liu, X.; Wen, D. Hydrological characteristics of Qinghai Lake, 1956–2017. *J. Hydroecol.* **2020**, *41*, 27–33.
37. Higgins, S.; Pennuto, C.; Howell, T.; Theodore, W.; Lewis, J.; Makarewicz, D. Urban influences on Cladophora blooms in Lake Ontario—ScienceDirect. *J. Great Lakes Res.* **2012**, *38*, 116–123. [CrossRef]
38. Liu, X.; Chen, Y.W. A review on the ecology of Cladophora. *J. Lake Sci.* **2018**, *30*, 881–896.
39. Hu, C.; Lee, Z.; Ma, R.; Yu, K.; Li, D.; Shang, S. Moderate resolution imaging spectroradiometer (MODIS) observations of cyanobacteria blooms in Taihu Lake, China. *J. Geophys Res. Ocean.* **2010**, *115*, C04002. [CrossRef]
40. Wang, S.; Li, J.; Zhang, B.; Spyrakos, E.; Tyler, A.N.; Shen, Q.; Zhang, F.; Kuster, T.; Lehmann, M.K.; Wu, Y.; et al. Trophic state assessment of global inland waters using a MODIS-derived Forel-Ule index. *Remote Sens. Environ.* **2018**, *217*, 444–460. [CrossRef]
41. Zhang, J.; Chen, L.Q.; Chen, X.L. Monitoring the cyanobacterial blooms based on remote sensing in Lake Erhai by FAl. *J. Lake Sci.* **2016**, *28*, 718–725.
42. Hu, M.Q.; Zhang, Y.C.; Ma, R.H.; Zhang, Y.X. Spatial and Temporal Dynamics of Floating Algal Blooms in Lake Chaohu in 2016 and Their Environmental Drivers. *Environ. Sci.* **2018**, *39*, 87–99.
43. Zhu, H.; Xiong, X.; Ao, H.; Wu, C.; He, Y.; Hu, Z.; Liu, G. Cladophora reblooming after half a century: Effect of climate change-induced increases in the water level of the largest lake in Tibetan Plateau. *Environ. Sci. Pollut. Res.* **2020**, *27*, 42175–42181. [CrossRef]
44. Cambridge, M.L.; Breeman, A.M.; Van den Hoek, C. Temperature responses and distribution of Australian species of Cladophora (Cladophorales: Chlorophyta). *Aquat. Bot.* **1991**, *40*, 73–90. [CrossRef]

45. Higgins, S.N.; Hecky, R.E.; Guildford, S.J. Environmental Controls of Cladophora Growth Dynamics in Eastern Lake Erie: Application of the Cladophora Growth Model (CGM). *J. Great Lakes Res.* **2006**, *32*, 629–644. [CrossRef]
46. Whitton, B.A. Biology of Cladophora in freshwaters. *Water Res.* **1970**, *4*, 457–476. [CrossRef]
47. Bellis, V.J.; McLarty, D.A. Ecology of Cladophora Glomerata (L.) KÜTZ in sourthern Ontario 1. *J. Phycol.* **2010**, *3*, 57–63. [CrossRef] [PubMed]
48. Higgins, S.N.; Howell, E.T.; Hecky, R.E.; Guildford, S.J.; Smith, R.E. The wall of green: The status of Cladophora glomerata on the northern shores of Lake Erie's eastern basin, 1995–2002. *J. Great Lakes Res.* **2005**, *31*, 547–563. [CrossRef]
49. Zhang, M.; Duan, H.; Shi, X.; Yu, Y.; Kong, F. Contributions of meteorology to the phenology of cyanobacterial blooms: Implications for future climate change. *Water Res.* **2012**, *46*, 442–452. [CrossRef]